GeoScienceWorld
Lithosphere
Volume 2023, Article ID lithosphere_2023_176, 11 pages
https://doi.org/10.2113/2023/lithosphere_2023_176

Lithosphere

Research Article

Geochemical Composition Variations and Tectonic Implications of the Baoligaomiao Formation Volcanic Rocks from the Uliastai Continental Margin, Southeast Central Asian Orogenic Belt

Jianzhou Tang,[1,2,3] **Zhicheng Zhang**,[2,3] **and Zejia Ji**[2,3]

[1]*College of Geology and Environment, Xi'an University of Science and Technology, Xi'an, China*
[2]*School of Earth and Space Sciences, Peking University, Beijing, China*
[3]*MOE Key Laboratory of Orogenic Belt and Crustal Evolution, Peking University, Beijing, China*

Correspondence should be addressed to Zhicheng Zhang; zczhang@pku.edu.cn

Received 19 April 2023; Accepted 29 September 2023; Published 30 October 2023

Academic Editor: Songjian Ao

The Permo-Carboniferous tectonic evolution in the Uliastai continental margin (UCM), north of the southeast central Asian Orogenic Belt, remains controversial. This work examined the geochemical composition of the felsic volcanic rocks from the lower and upper part of the Baoligaomiao Formation in the UCM. Zircon U-Pb ages reveal that the Baoligaomiao Formation has a long-lived eruption duration, from ca. 285 to 328 Ma. The lower part (ca. 328–310 Ma) of the Baoligaomiao Formation is dominated by clastic and pyroclastic rocks with subordinate intermediate-felsic volcanic rocks, whereas the upper part (ca. 307–285 Ma) mainly consists of felsic volcanic rocks and pyroclastic rocks. Calculations reveal that the felsic volcanic rocks from the lower part have low zircon saturation temperatures (T_{Zr} = 747°C–795°C), whereas those from the upper part exhibit high T_{Zr} (ca. 793°C–930°C). Zircons from the lower part exhibit high $\varepsilon_{Hf}(t)$ values and $^{176}Lu/^{177}Hf$ ratios, in contrast to the low $\varepsilon_{Hf}(t)$ values and $^{176}Lu/^{177}Hf$ ratios of zircons from the upper part. Those petrogeological and geochemical shifts might support the tectonic switch model in the UCM at the end of the Carboniferous, providing new constraints on the Late Carboniferous closure of the Hegenshan Ocean.

1. Introduction

The Central Asian Orogenic Belt is one of the largest fossil accretionary orogenic belt worldwide [1], which is surrounded by Siberian Craton in the north and North China and Tarim Craton in the south (Figure 1(a)). There is a controversy on the Permo-Carboniferous tectonic evolution of the Uliastai continental margin (UCM) in the southeast Central Asian Orogenic Belt (SE CAOB; Figure 1(b)) [2–4]. This dispute might be diffused by the two phases of rift-related volcanism from the Baoligaomiao Formation in the UCM. Some scholars argue that the two phases of rift-related volcanism are formed in different tectonic settings, the former is subduction-related, and the latter is post-accretionary/collision-related [4–7]. Alternatively, others suggest two phases of rift-related volcanism are continuous, indicating a long-lived rifting process from Late Carboniferous to Early Permian [2, 8]. Thus, it is important to examine the differences between the two phases of volcanic rocks, exploring whether there was a tectonic switch during the end of the Carboniferous.

The Baoligaomiao Formation volcanism in the UCM has a long-lived eruption duration from Late Carboniferous to Early Permian [6, 9–13]. Rock association and whole-rock geochemistry variations of this formation have been identified and used to delineate the tectonic switch in the UCM [4, 6]. Recent studies indicate that the joint using of zircon U-Pb and Hf isotope data can also infer a regional tectonic evolution [14, 15]. Zircon $^{176}Lu/^{177}Hf$ ratios were sensitive proxies of magma crystallization pressure; zircon crystallizes deeper have low $^{176}Lu/^{177}Hf$ ratios, whereas those crystallizes shallower have high $^{176}Lu/^{177}Hf$ ratios [14]. In

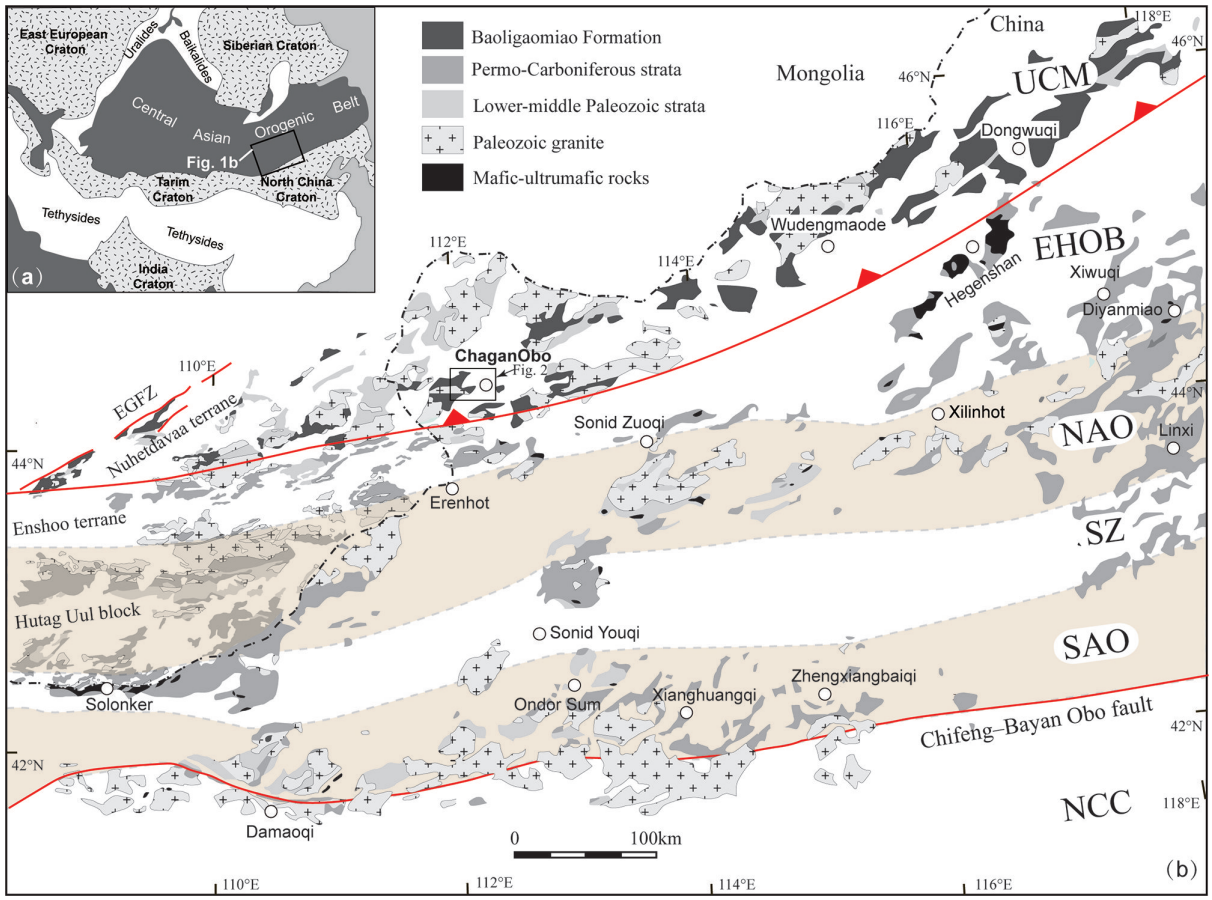

FIGURE 1 (a) Tectonic framework of the Central Asian Orogenic Belt. (b) Simplified geological map showing the Baoligaomiao Formation volcano-sedimentary rocks in the UCM [5, 9–11]. EGFZ: East Gobi fault zone; NCC: North China Craton; SAO: South accretionary orogen; SZ: Solonker zone; NAO: North accretionary orogen; EHOB: Erenhot-Hegenshan ophiolite belt; UCM: Uliastai continental margin.

addition, zircon $\varepsilon_{Hf}(t)$ values are mainly restrained by the relative input of depleted mantle and crustal components [15, 16]. Thus, zircons from the Baoligaomiao Formation volcanic rocks are potential proxies to explore the Permo-Carboniferous tectonic evolution of the UCM.

In this contribution, this work presented and compiled zircon U-Pb and Lu-Hf isotope, and whole-rock elements data of the Baoligaomiao Formation volcanic rocks to explore whether there was a tectonic switch in the UCM at the end of Carboniferous.

2. Geological Background

2.1. Southeast Central Asian Orogenic Belt. Five tectonic units have been divided in the SE CAOB (Figure 1b), from north to south, the UCM, Hegenshan-Erenhot ophiolite belt (EHOB), North accretionary orogen (NAO), Solonker zone (SZ), and Southern accretionary orogen (SAO).

Two episodic spreading events have been identified in the SZ, featured by abundant mafic-ultramafic rocks [3, 17–19]. The NAO and SAO have Cambrian to Early Devonian arc magmatic rocks, which recorded the subduction of the Paleo-Asian Ocean along the SZ [18, 19]. Following a ca. 50 Ma magmatic and depositional hiatus, the NAO was reactivated by Late Carboniferous and Early Permian magmatism, whereas the SAO was dominated by carbonate-clastic deposition. The Paleo-Asian Ocean closed at the end of the Permian, implying the final suture of the CAOB [20].

The EHOB documented the spreading and subduction of the Hegenshan Ocean, distinguished by the Carboniferous mafic-ultramafic rocks [3, 21]. Those mafic-ultramafic rocks were covered by Permian sedimentary rocks [22]. Silurian and Devonian limestones, mudstone, and siltstone from the UCM indicate a passive continental margin deposition environment [23]. In the Early Carboniferous, the UCM switched into an active continental margin setting caused by the northward subduction of the Hegenshan Ocean [24]. The passive continental margin deposition was covered by the Hongaobao Formation and Baoligaomiao Formation volcano-clastic deposition [2, 23].

2.2. Baoligaomiao Formation. The Baoligaomiao Formation, or called as Baolige Formation, is mainly distributed along the ChaganObo-Dongwuqi areas in the UCM [9, 11, 12, 25, 26]. This formation is a suite of volcano-clastic deposition (Figure 2(a)–2(c)), consisting of andesite, rhyolite, pyroclastic rock, mudstone, siltstone, and sandstone [13, 26]. The lower part of the Baoligao-

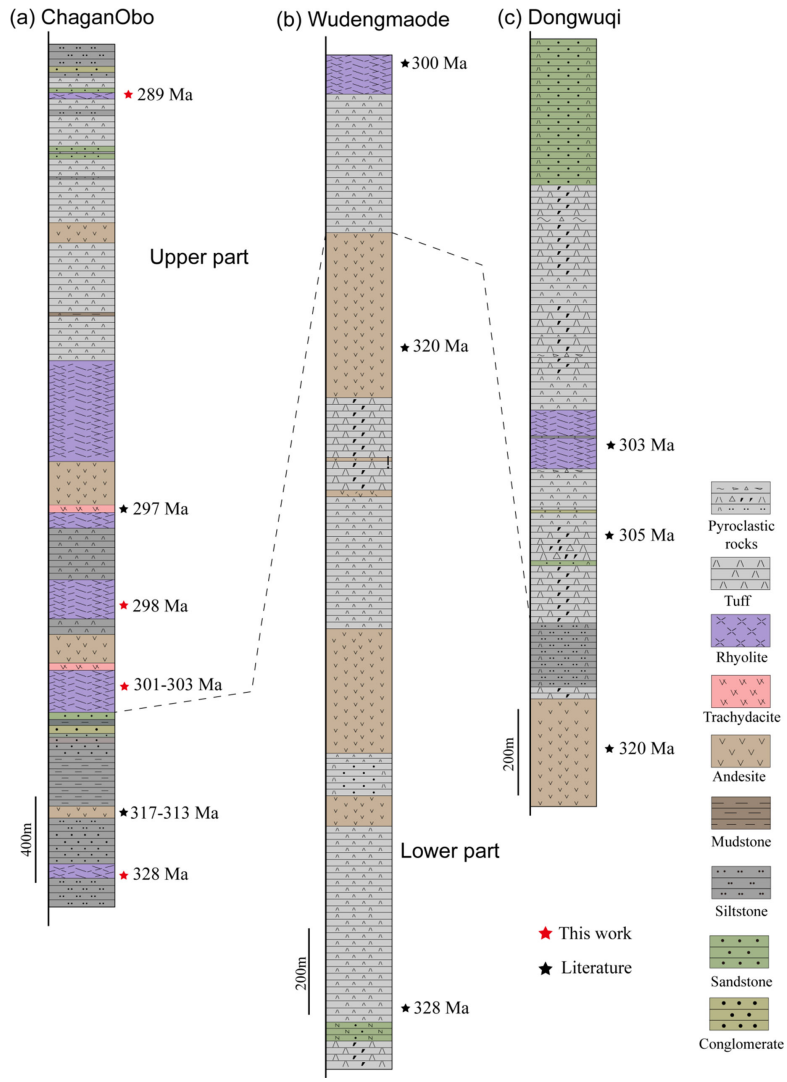

FIGURE 2 Stratigraphic sequences of the Baoligaomiao Formation from ChaganObo [26], Wudengmaode [25], and Dongwuqi [9]. Age data is from references [6, 9, 25] and this work.

miao Formation from the Wudengmaode area has a large volume of pyroclastic rocks and andesite (Figure 2(b)), whereas other areas (e.g., ChaganObo and Dongwuqi) were dominated by clastic deposition (Figure 2(a) and 2(c)). The upper part is mainly composed of rhyolite and pyroclastic rock [9, 10]. In the east of the Dongwuqi area, the Baoligaomiao Formation is sporadically exposed and dominated by clastic deposition [9]. Plant fossils from the Baoligaomiao Formation imply an Upper Carboniferous to Lower Permian depositional age [9]. In accordance with the fossil records, zircon dating results also gave Permo-Carboniferous ages [9, 25, 26].

Eighteen volcanic rock samples, including 2 andesitic, 2 dacitic, and 13 rhyolitic volcanic rock samples, were collected from the Baoligaomiao Formation in the ChaganObo area (Figure 2 and Figure 3). The andesitic rocks are brown in color (Figure 4(a)), whereas the rhyolitic and dacitic rocks are yellowish-white (Figure 4(b)). Phenocrysts of rhyolite samples mainly consist of quartz, alkaline-feldspar, and plagioclase (Figure 4(c) and 4(d)). In addition, biotite phenocrysts were observed in rhyolite sample NM18-140 (Figure 4(e)). The phenocryst of andesitic rock samples was mainly composed of plagioclase with subordinate hornblende (Figure 4(f)).

3. Materials and Methods

Eighteen volcanic rock samples were selected for whole-rock elements geochemistry analysis. Among them, six samples were dated and conducted to zircon Lu-Hf isotope analysis.

Zircon U-Pb dating of volcanic rock samples was conducted on the laser ablation-inductively coupled plasma mass spectrometry (LA-ICP-MS) with frequency of 10 Hz and a beam of 32 μm at the School of Earth and Space Sciences, Peking University (SESS-PKU). Harvard sample 91,500 (ca. 337 Ma) was used as a reference. Detailed procedures can be found in Sun et al. [27]. In-situ zircon Lu-Hf isotope analysis using MC-ICP-MS (Neptune) equipped with a New Wave UP213 laser ablation system

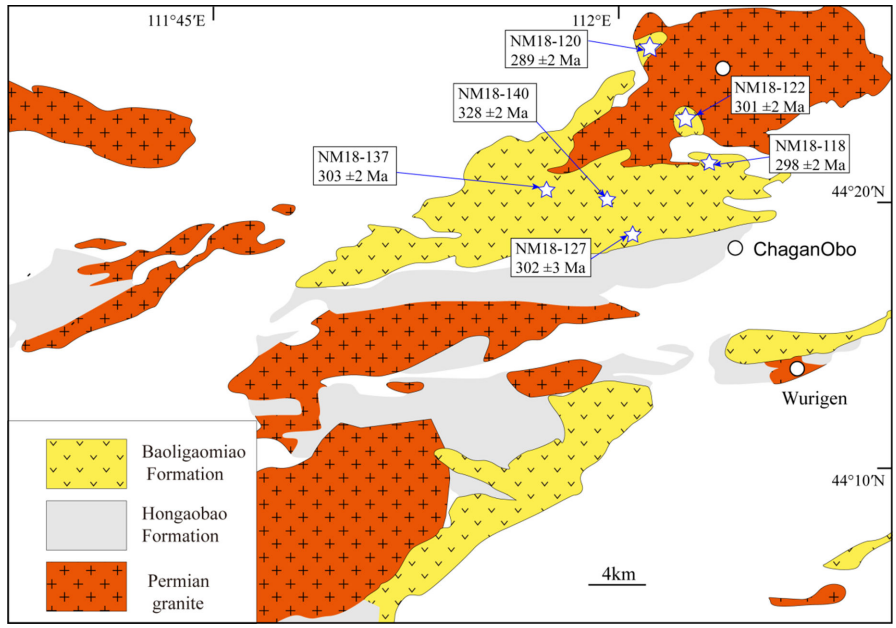

Figure 3 Simplified geological map of the ChaganObo area showing the sample locations [7].

at the SESS-PKU. The spot size of Lu-Hf analysis was ca. 44 μm, and the zircon Plešovice was the reference ($^{176}Hf/^{177}Hf$ = 0.282482 ± 13). Detailed analytical procedures can be found in Zhang, Ireland, Zhang, GaoandSong [28].

The whole-rock elemental geochemistry was conducted at the SESS-PKU. Whole-rock major elements were analyzed on X-ray fluorescence spectrometer, and the trace elements were analyzed on Agilent 7500 inductively coupled plasma mass. The analytical procedures are the same as those of Sun et al. [27]. The analytical uncertainty of the major elements was ±1%, whereas that of the trace elements was ±5%.

4. Results

4.1. Zircon U-Pb Ages. The analyzed zircons are euhedral and long-columnar (Figure 5). They show oscillatory zones and high Th/U ratios (>0.32). These features indicate that they are of magmatic origin. Zircon dating results were documented in online supplementary table S1, and the weighted mean ages reveal the dated Baoligaomiao Formation volcanic rocks formed at ca. 328–289 Ma.

Forty zircon grains from rhyolite sample NM18-140 were analyzed, and 38 of them were concordant. Apart from two grains showing young $^{206}Pb/^{238}U$ ages (305 and 309 Ma), the other 36 grains gave a weighted mean age of 328 ± 2 Ma (Figure 5(a)). The very few young-concordant and discordant ages could be caused by the Pb-loss resulting from the hydrothermal alteration [29].

Forty zircon grains from rhyolite sample NM18-118 were analyzed, and 36 of them are concordant. The 35 youngest analyses gave a weighted mean age of 298 ± 2 Ma (Figure 5(b)). The old age of 321 Ma could be from the captured zircon.

Thirty-one zircon grains from rhyolite sample NM18-120 were analyzed, and 29 of them were concordant. The 29 analyses gave a weighted mean age of 289 ± 2 Ma (Figure 5(c)).

Thirty-nine zircon grains from rhyolite sample NM18-122 were analyzed, and all of them were concordant. The 39 analyses gave a weighted mean age of 301 ± 2 Ma (Figure 5(d)).

Thirty zircons from sample NM18-127 were analyzed, and 20 of them were concordant. Most of the analyses (n = 18) exhibited similar $^{206}Pb/^{238}U$ ages of 295–310 Ma, with a weighted mean age of 302 ± 3 Ma (Figure 5(e)). In addition, one young $^{206}Pb/^{238}U$ age of 275 Ma and one old $^{206}Pb/^{238}U$ age of 341 Ma were also obtained. The youngest concordant age (275 Ma) could be related to hydrothermal alteration [29].

Forty-one grains from rhyolite sample NM18-137 were analyzed, and 37 of them were concordant. Thirty-six youngest concordant analyses gave a weighted mean age of 303 ± 2 Ma (Figure 5(f)), and the other grain has an old $^{206}Pb/^{238}U$ age of 351 Ma.

4.2. Whole-Rock Geochemistry. The whole-rock geochemistry data can be found in online supplementary table S2. Except for two andesite samples with high loss-on-ignition (3.16 and 3.53 wt.%), other rhyolite and dacite samples show low loss-on-ignition (LOI < 2.52 wt.%).

Rhyolite sample NM18-140 from the lower part of the Baoligaomiao Formation exhibits high SiO_2 (74.17 wt.%), Al_2O_3 (12.72 wt.%), Na_2O (4.39 wt.%), and K_2O (4.07 wt.%) contents and low TFe_2O_3 (1.08 wt.%), MgO (0.28 wt.%), and TiO_2 (0.29 wt.%) contents. This sample plots within the subalkaline field and belongs to medium-K calc-alkaline (Figure 6(a) and 6(b)). In the N-MORB (normal middle ocean ridge basalt) normalized spider diagrams, they show significant Ba-Sr-Eu and Nb-Ta negative anomalies (Figure 7(a)). The negative Eu anomaly

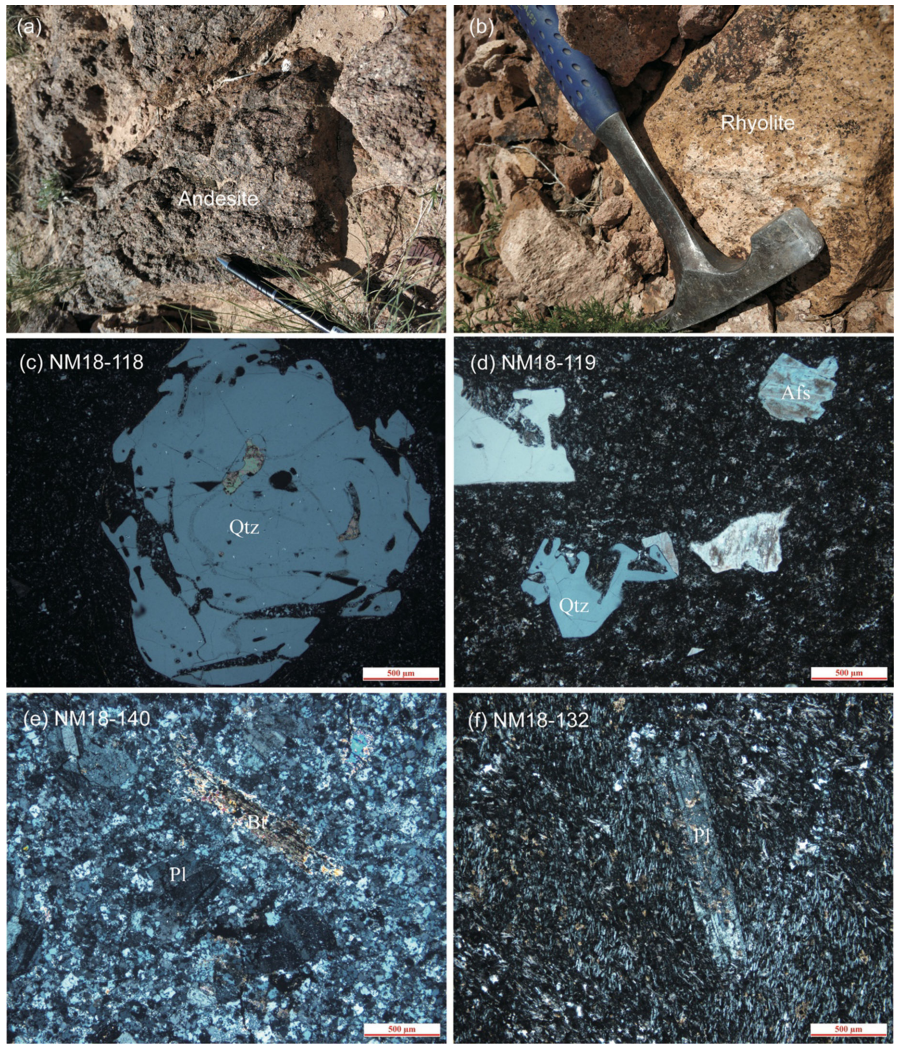

FIGURE 4 Representative photos from outcrops (a–b) and microscope (c–f). Figures 4(c)–4(e) are from rhyolite samples, and Figure 4(f) is from an andesite sample. Qtz: quartz; Pl: plagioclase; Afs: alkali feldspar; Bt: biotite.

can also be observed in the Chondrite-normalized rare earth elements pattern (Figure 7(b)).

The volcanic rocks from the upper part of the Baoligaomiao Formation are dominated by rhyolite and dacite with subordinate andesitic rocks (Figure 6(a)). Except for two andesite samples that have low SiO_2 contents (57.71 and 58.51 wt.%), other samples show high SiO_2 (64.47, 81.95 wt.%) contents. Likewise, the andesitic samples exhibit high TFe_2O_3 (7.55 and 9.46 wt.%), MgO (2.42 and 2.66 wt.%), and CaO (2.47 and 4.95 wt.%) contents, whereas dacite and rhyolite samples have relatively low contents of TFe_2O_3 (0.18, 5.40 wt.%), MgO (0.13, 1.45 wt.%), and CaO (0.02, 1.82 wt.%). The K_2O+Na_2O contents of the Baoligaomiao Formation volcanic rock samples range from 5.24 to 9.83 wt.%, and most of them plot within the subalkaline field (Figure 6(a)). The andesitic samples belong to the medium-K calc-alkaline series, whereas the rhyolitic samples are variable in the K_2O contents (Figure 6(b)). The dacite and rhyolite samples have similar trace elements and rare earth element patterns, with distinct Nb-Ta and Sr negative anomalies and variable Ba and Eu anomalies (Figure 7(c) and 7(d)). In contrast, the andesite samples show no negative Ba-Sr-Eu anomalies in the N-MORB normalized trace elements pattern, but negative Nb-Ta anomalies can be identified (Figure 7(c) and 7(d)).

4.3. Zircon Lu-Hf Isotopes. Five samples were selected for zircon Lu-Hf analysis, and all of them show depleted Hf isotopic composition, see online supplementary table S3.

Eight zircons from rhyolite sample NM18-120 were analyzed. Among them, seven grains have high $^{176}Yb/^{177}Hf$ values (>0.1). All of them show low $^{176}Lu/^{177}Hf$ ratios (0.002, 0.005) and positive $\varepsilon_{Hf}(t)$ values (+12.67 to +20.14).

Six zircons from rhyolite sample NM18-118 exhibit high $^{176}Yb/^{177}Hf$ values (>0.1) and $^{176}Lu/^{177}Hf$ ratios (0.004, 0.006), and positive $\varepsilon_{Hf}(t)$ values (+6.23 to +13.36).

Ten zircons from rhyolite sample NM18-122 show low $^{176}Lu/^{177}Hf$ ratios (0.001, 0.003). Among them, eight grains show low $^{176}Yb/^{177}Hf$ values (<0.1) and positive $\varepsilon_{Hf}(t)$ values (+7.56 to +14.81).

Nine zircons from rhyolite sample NM18-137 show low $^{176}Lu/^{177}Hf$ ratios (0.001, 0.003), and eight of them exhibit

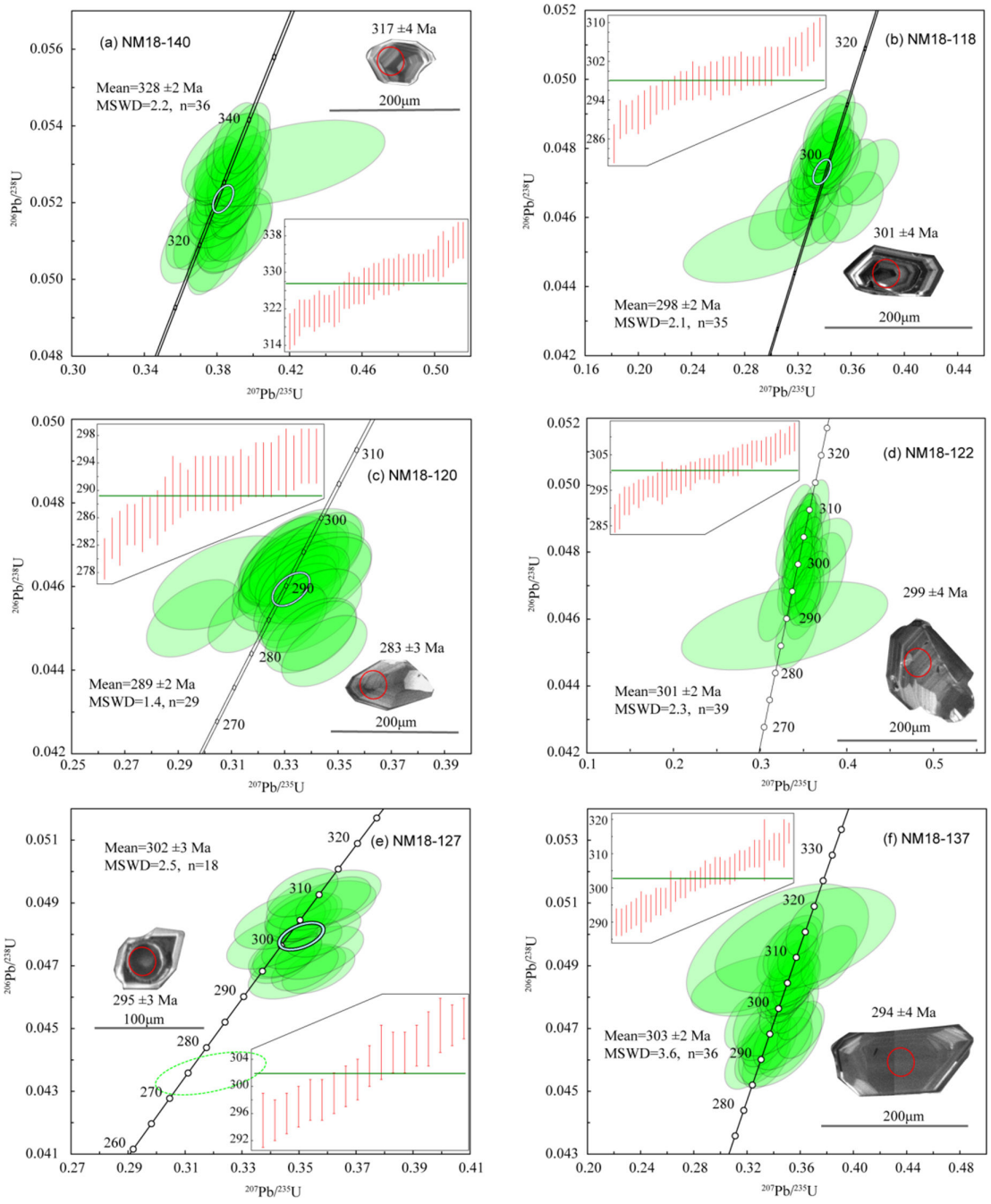

FIGURE 5 Zircon U-Pb concordant plots for the rhyolite samples from the Baoligaomiao Formation.

low $^{176}Yb/^{177}Hf$ values (< 0.1). The eight grains exhibit positive $\varepsilon_{Hf}(t)$ values (+8.34 to +16.80).

Seven zircons from rhyolite sample NM18-140 have low $^{176}Lu/^{177}Hf$ ratios (0.002, 0.004), and five of them exhibit low $^{176}Yb/^{177}Hf$ ratios (< 0.1). The five grains have positive $\varepsilon_{Hf}(t)$ values (+10.22 to +14.99).

Except for zircon grains from samples NM18-120 and NM18-118 have high $^{176}Yb/^{177}Hf$ ratios (>0.1), most zircons from the other three samples have low $^{176}Yb/^{177}Hf$ ratios. Therefore, it should be cautious when using the $\varepsilon_{Hf}(t)$ values from samples NM18-120 and NM18-118.

5. Discussion

5.1. Petrogenesis of the Volcanic Rocks. All rhyolite samples from Baoligaomiao Formation show negative Sr-Ba-Eu anomalies (Figure 7), indicating the fractional crystallization of feldspars. This is consistent with the observations of plagioclase and alkali-feldspars phenocrysts under the microscope.

Rhyolite sample NM18-140 from the lower sequence of the Baoligaomiao Formation has a high Ga/Al ratio and Zr+Nb+Ce+Y content, plotting within the A-type field

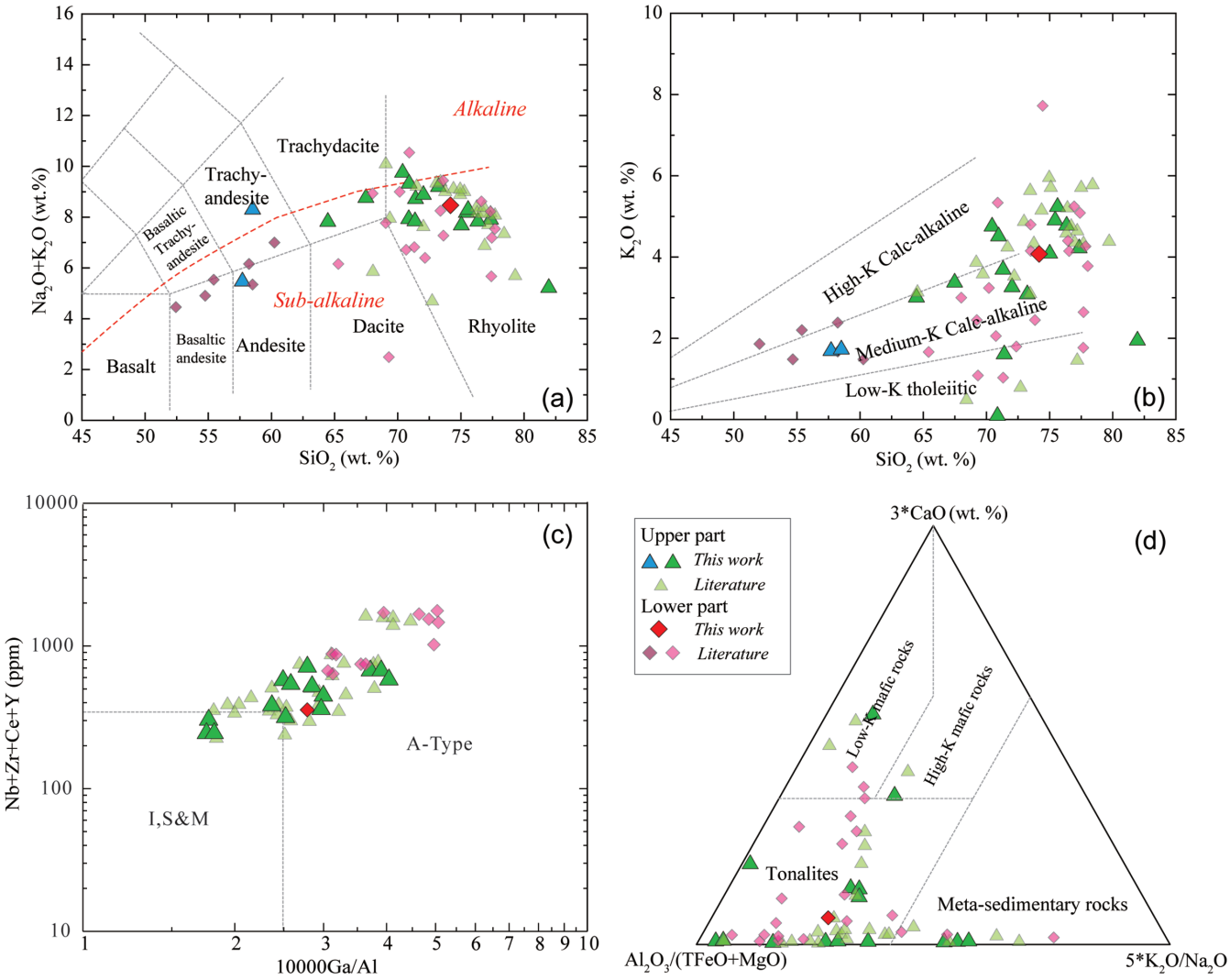

FIGURE 6 Binary diagrams of (a) SiO_2 versus Na_2O+K_2O [33], (b) SiO_2 versus K_2O [34], and (c) 10000Ga/Al versus Nb+Zr+Ce+Y [35] and ternary diagram of Al_2O_3/(TFeO+MgO)-5*K_2O/Na_2O-3*CaO [36].

(Figure 6(c)). The A-type rhyolites have also been identified in the south of the ChaganObo area [6]. In addition, calculations suggest that the sample NM18-140 shows high zircon saturation temperatures of 826°C [30]. The A-type rhyolite might be derived from the melting of underplated mafic rocks or juvenile crust, as indicated by the depleted zircon Hf isotopic composition. However, in the ternary diagram, this sample overlaps with the partial melts of tonalites (Figure 6(d)). Thus, the precursor of sample NM18-140 is the partial melt of the juvenile felsic crust.

Except for three samples (NM18-118, NM18-127, and NM18-138) plotting within I, S, and M type field, most rhyolite samples from the upper part also show high Ga/Al ratios and Zr+Nb+Ce+Y contents, implying the affinities of A-type granites (Figure 6(c)). Likewise, the three samples with low Ga/Al ratios show relatively low zircon saturation temperatures (784°C, 809°C, and 816°C), in contrast to the high zircon saturation temperatures (827°C, 914°C) from other samples with high Ga/Al ratios [30]. In the ternary diagram, the three samples exhibit low K_2O/Na_2O ratios and overlap with the partial melts of mafic rocks or tonalites, while other samples with high Ga/Al ratios overlap with the partial melts of igneous rocks (mafic rocks and tonalities) and meta-sedimentary rocks (Figure 6(d)). Thus, most of the samples belong to the A-type rhyolite with subordinate I-type or I/A-type rhyolite. In any case, these rhyolite samples have depleted zircon Hf isotopic composition, indicative of the juvenile protolith.

Andesite samples from the upper part of the Baoligaomiao Formation show negative Nb-Ta anomalies, meaning the partial melts from the metasomatized lithospheric mantle without the breakdown of rutile [31]. Enrichments of large ion lithophile elements and light rare earth elements suggest the involvement of fluids and/or melts from the subducted oceanic slab.

5.2. Tectonic Implications. The Baoligaomiao Formation has a long-lived eruption duration, mainly from ca. 328 to 285 Ma (Figure 8(a)), which recorded the tectonic evolution of the UCM [5, 6]. Volcanic rocks from the lower part have

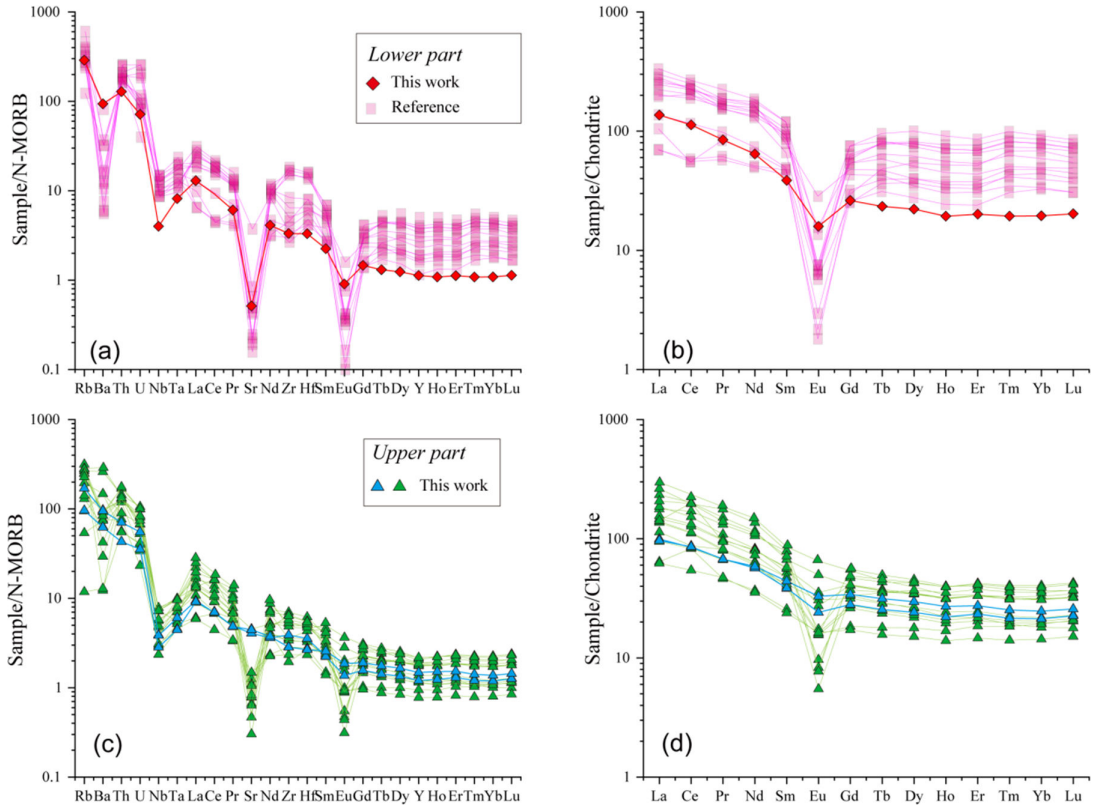

FIGURE 7 N-MORB (normal-middle ocean ridge basalt) normalized spider diagrams and Chondrite-normalized REE patterns for the Baoligaomiao Formation volcanic rocks. The normalization values are from Reference 37. The lower part of the Baoligaomiao Formation rhyolite samples are from Reference 6.

U-Pb ages of ca. 310–328 Ma, whereas those from the upper part have U-Pb ages of ca. 307–285 Ma.

The A-type rhyolites are found in both the lower and upper part of the Baoligaomiao Formation [6]. Therefore, the Baoligaomiao Formation erupted at an extensional tectonic setting. However, there are some differences between the volcanic rock association, which have been linked with the switch of tectonic setting [5, 6]. In the lower part, the volcanic rocks are dominated by andesite, while the andesite is minor in the upper part [6, 9]. Although both the A-type and I-type felsic volcanic rocks occurred both in the Upper Carboniferous and Lower Permian, the Upper Carboniferous were dominated by I-type rocks and the Lower Permian mainly consisted of A-type rocks [4].

Our compilation suggests that zircon saturation temperatures (T_{Zr}) and Lu-Hf isotopic composition from the felsic rocks show a significant shift at ca. 310–305 Ma (Figure 8(b)–8(d)). Felsic volcanic rocks from the lower part have low average T_{Zr} (ca. 747°C–795 °C), contrasting to the high average T_{Zr} (ca. 793°C–930 °C) of felsic rocks from the upper part. Although the increase of the zircon saturation temperatures (Figure 8(b)) and the volume of A-type felsic rocks can be linked with a long-lived rifting process, the shifts of zircon $^{176}Lu/^{177}Hf$ ratios and $\varepsilon_{Hf}(t)$ values disagree with this model (Figure 8(c) and 8(d)). Moreira et al. [14] suggest that the zircons with low $^{176}Lu/^{177}Hf$ ratios could be crystallized at a compressional tectonic setting, whereas those with high $^{176}Lu/^{177}Hf$ ratios crystallized at an extensional tectonic setting. However, the explanation of Moreira et al. [14] might not be well matched with the scenario of the UCM, as the presence of A-type rhyolite both in the upper and lower part. Instead, the lower zircon $^{176}Lu/^{177}Hf$ ratios from the upper part of the Baoligaomiao Formation might imply a more thickened crust origin, consistent with the decrease in zircon $\varepsilon_{Hf}(t)$ values, which has been linked with the collision of arc/continent and continent and more involvement of crustal materials [15, 16].

Ophiolites (with a U-Pb age of ca. 336 Ma) from Diyanmiao have similar petrology and geochemistry nature to those from Izu-Bonin-Mariana, and northward subduction initiation of the Hegenshan Ocean has been proposed [24]. The northward subduction of the Hegenshan Ocean would construct continental arcs in the UCM along with the slab descending and formation of mantle wedge [24, 32]. Basaltic andesite and andesite (ca. 326–314 Ma) from the lower part of the Baoligaomiao Formation in the south of ChaganObo are enriched in large ion lithophile elements and light rare earth elements and depleted in high field-strength elements, which represent the Early Carboniferous subduction-related, mature, continental arc volcanism [5, 6]. The ChaganObo A-type rhyolite (ca. 326–318 Ma) from the lower part was also subduction-related, indicative of local extension caused by trench retreat [5, 6]. Monzogranites and granite porphyries with age of ca. 336–320 Ma from Wudengmaode belong to the

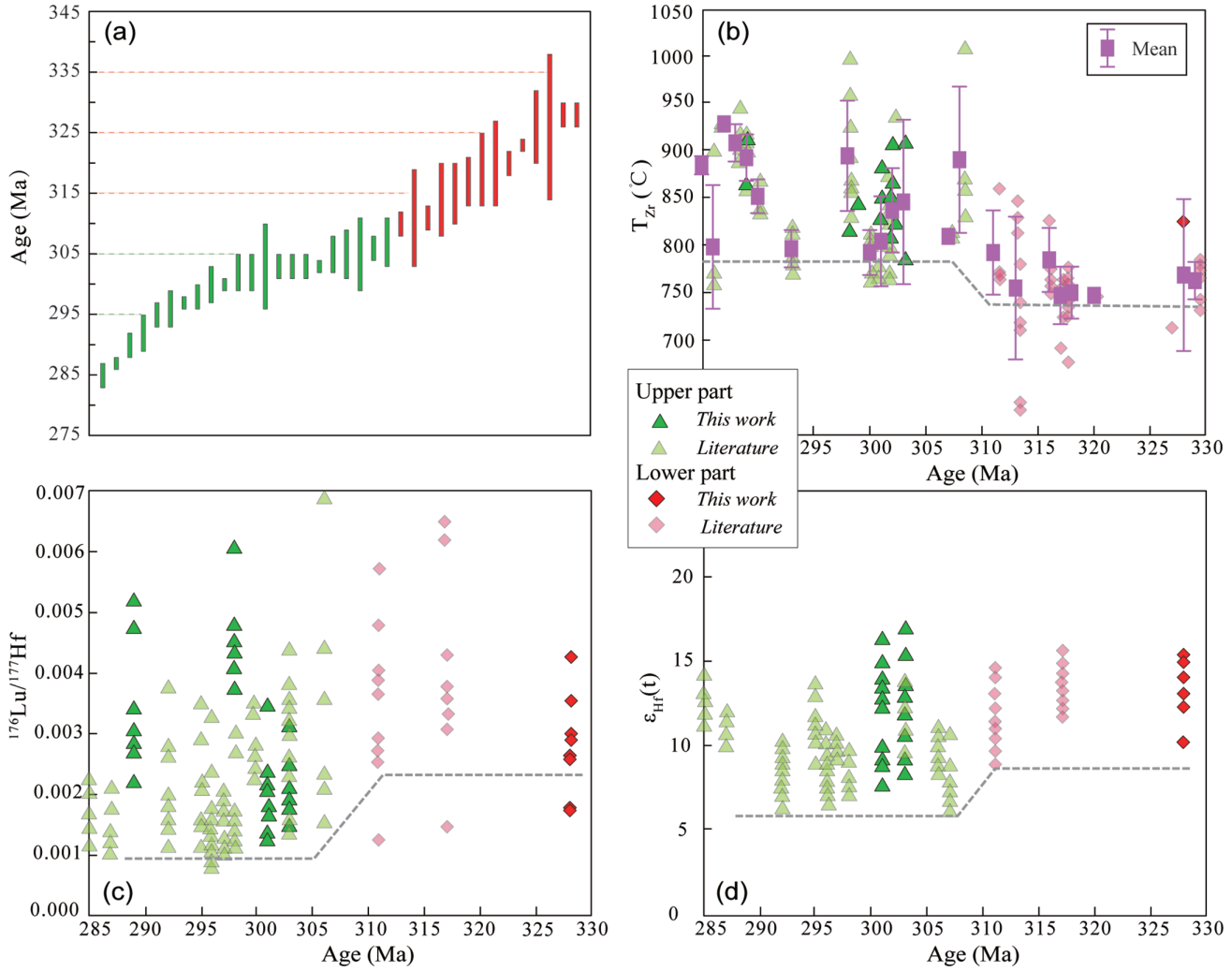

FIGURE 8 Plots of (a) eruption ages of the volcanic rocks from Baoligaomiao Formation, and (b) T_{Zr} and (c–d) zircon Lu-Hf isotopic ratios variations through time. Data are from this work and references 4–6, 9, 13, 25, 26.

calc-alkaline I-type granites and are generated by the partial melting of juvenile crust in a north-dipping subduction-related environment [4]. The lower volcanic rocks from the Baoligaomiao Formation show relatively uniform zircon Hf isotopic compositions, which could mean minor involvement of crustal materials during the nascent subduction [32]. The low T_{Zr} (ca. 747°C–795°C) from the lower part of the Baoligaomiao Formation is compatible with the continental arc environment [6]. Those observations might indicate the lower part of the Baoligaomiao Formation erupted in a continental arc environment.

Although there are andesites in the upper part of the Baoligaomiao Formation, which are minor and have been explained as the partial melting of the metasomatized lithosphere mantle during the post-collision or post-accretionary extensional setting [6]. Field investigations show that the mafic-ultramafic rocks are unconformably covered by the Lower Permian Gegenaobao Formation in the Hegenshan area, and a Late Carboniferous emplacement timing of the ophiolites from the EHOB was proposed [22]. Provenance analyses from the Lower Permian sandstones reveal that the north of the Sonid Zuoqi area received multiple detritus from Mongolia arcs, NAO, and microcontinents [23]. The magmatic gap at ca. 314–307 Ma in the EHOB has been linked with the closure of the Hegenshan Ocean [4, 7]. An undeformed dioritic dike with the age of ca. 314 Ma intruded the highly deformed Carboniferous strata in the south of ChaganObo [21]. In addition, the hybridization of the cold-water flora and warm-water flora was identified in the upper part of the Baoligaomiao Formation, implying the Hegenshan Ocean was not a significant geographical barrier at that time [9]. Early Permian rift basins in the UCM and EHOB were regarded as the products of post-collision/accretionary extension [2, 23]. The high T_{Zr} (ca. 793°C–930°C) from the upper part of Baoligaomiao Formation is also consistent with an extensional setting. Hence, it is reliable that the upper part of Baoligaomiao Formation was generated in a post-accretionary extensional setting.

In summary, the petrogeology and geochemistry differences between the lower and upper part of the Baoligaomiao Formation volcanic rocks could be consistent

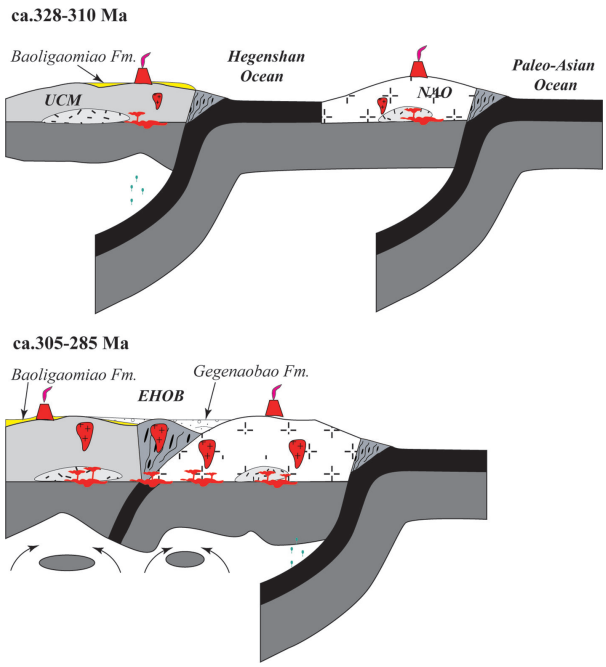

Figure 9 Tectonic switch model in the UCM and EHOB. NAO: North accretionary orogen; EHOB: Erenhot-Hegenshan ophiolite belt; UCM: Uliastai continental margin.

with the previous inferences [4, 6, 7], supporting a tectonic switch model, from the Carboniferous subduction to the Early Permian post-accretionary extension (Figure 9).

6. Conclusions

Whole-rock geochemistry and zircon U-Pb and Lu-Hf isotope data from the Baoligaomiao Formation felsic volcanic rocks provide new insights into the Permo-Carboniferous tectonic switch in the UCM. A compiled zircon U-Pb age dataset suggests that the Baoligaomiao Formation volcanism has a long-lived eruption duration from ca. 328 to 285 Ma. The differences in zircon Hf isotope and whole-rock geochemistry between the lower and upper part of the Baoligaomiao Formation felsic volcanic rocks support a tectonic switch model from the Carboniferous subduction to the Early Permian post-accretionary extension.

Data Availability

The data of this study is available in the supplementary material.

Conflicts of Interest

The authors declare that they have no conflicts of interest.

Acknowledgments

We thank two anonymous reviewers for their constructive comments, which led to significant improvements in the quality of our paper. This work was financially supported by the National Key Research and Development Project of China (2017YFC0601302), SINOPEC Petroleum Exploration and Production Research Institute (8410102109) and the National Natural Science Foundation of China (42102128).

Supplementary Materials

Supplementary table 1: Zircon U-Pb dating results from the Baoligaomiao Formation volcanic rocks. Supplementary table 2: Major and trace elements contents from the Baoligaomiao Formation volcanic rocks. Supplementary table 3. Zircon Hf isotopic composition of the Baoligaomiao Formation volcanic rocks.

References

[1] W. Xiao, B. F. Windley, S. Sun, et al, "A tale of amalgamation of three Permo-Triassic collage systems in central Asia: Oroclines, Sutures, and terminal accretion, " *Annual Review of Earth and Planetary Sciences*, vol. 43, no. 1, pp. 477–507, 2015.

[2] Z. Ji, Z. Zhang, J. Yang, Y. Chen, and J. Tang, "Carboniferous–early Permian sedimentary rocks from the North-Eastern Erenhot, North China: implications on the Tectono-Sedimentary evolution of the South-Eastern central Asian Orogenic belt, " *Geological Journal*, vol. 55, no. 3, pp. 2383–2401, 2020.

[3] S. Song, M.-M. Wang, X. Xu, et al., "Ophiolites in the Xing'An-inner Mongolia Accretionary belt of the CAOB: implications for two cycles of Seafloor spreading and Accretionary Orogenic events," *Tectonics*, vol. 34, no. 10, pp. 2221–2248, 2015.

[4] Z. G. Wang, K. Li, Z. C. Zhang, Y. Chen, and X. D. Wang, "Carboniferous to early Permian Magmatism in the Uliastai Continental margin (inner Mongolia) and its correlation with the Tectonic evolution of the Hegenshan ocean," *Lithos*, vols. 414–415, p. 106635, 2022.

[5] H. Chai, Q. Wang, J. Tao, M. Santosh, T. Ma, and R. Zhao, "Late Carboniferous to early Permian Magmatic pulses in the Uliastai Continental margin linked to slab rollback: implications for evolution of the central Asian Orogenic belt," *Lithos*, vols. 308–309, pp. 134–158, 2018.

[6] R. Wei, Y. Gao, S. Xu, et al., "The volcanic succession of Baoligaomiao, central inner Mongolia: evidence for Carboniferous Continental arc in the central Asian Orogenic belt," *Gondwana Research*, vol. 51, pp. 234–254, 2017.

[7] J. Tang, J. Cheng, Z. Zhang, et al., "Age, origin and Tectonic implications of late Carboniferous-early Permian Felsic Magmatic rocks from central inner Mongolia, South-Eastern central Asian Orogenic belt," *International Geology Review*, vol. 64, no. 9, pp. 1226–1247, 2022.

[8] Z. L. Yang, X. H. Zhang, and L. L. Yuan, "Construction of an island arc and back-arc Basin system in Eastern central Asian Orogenic belt: insights from contrasting late Carboniferous intermediate intrusions in central inner Mongolia, North China," *Lithos*, vols. 372–373, p. 105672, 2020.

[9] H. T. Xin, X. J. Teng, and Y. H. Cheng, "Stratigraphic subdivision and Isotope Geochronology study on the Baoligaomiao formation in the east Ujimqin County, inner

Mongolia," *Geological Survey and Research*, vol. 34, no. 1, pp. 1–9, 2011.

[10] F. B. He, B. Wei, J. X. Xu, Y. H. Sun, and R. J. Li, "Ages, origin and geological implications of the volcanic rocks in the Baoligaomiao formation of East Ujimqin banner, inner Mongolia," *Geology in China*, vol. 44, no. 6, pp. 1159–1174, 2017.

[11] K. Li, Z. C. Zhang, Z. S. Feng, et al, "Zircon SHRIMP U-PB dating and its geological significance of the late-Carboniferous to early-Permian volcanic rocks in Bayanwula area, the central of inner Mongolia," *Acta Petrologica Sinica*, vol. 30, no. 7, pp. 2041–2054, 2014.

[12] W. G. Li, "The timing of the Baolige formation," *Journal of Stratigraphy*, vol. 1, pp. 46–49, 1981.

[13] S. W. Huang, "Isotopic chronology of Volcanics of the Baoligaomiao formation in central and Eastern inner Mongolia," *Global Geology*, vol. 40, no. 3, pp. 475–496, 2021.

[14] H. Moreira, A. Buzenchi, C. J. Hawkesworth, and B. Dhuime, "Plumbing the depths of Magma crystallization using 176Lu/177Hf in Zircon as a pressure proxy," *Geology*, vol. 51, no. 3, pp. 233–237, 2023.

[15] N. J. Gardiner, C. L. Kirkland, and M. J. Van Kranendonk, "The juvenile Hafnium Isotope signal as a record of Supercontinent cycles," *Scientific Reports*, vol. 6, 2016.

[16] X. R. Zhang, G. C. Zhao, Y. G. Han, and M. Sun, "Differentiating advancing and retreating Subduction zones through regional Zircon HF Isotope mapping: A case study from the Eastern Tianshan, NW China," *Gondwana Research*, vol. 66, pp. 246–254, 2019.

[17] J. Tang, Z. Zhang, J. Xue, B. Liu, Y. Chen, and S. Zhang, "Permo-Carboniferous provenance shifts at the northern margin of the North China Craton and their Tectonic implications: Detrital Zircon U–PB–HF records from central inner Mongolia," *Gondwana Research*, vol. 95, pp. 134–148, 2021.

[18] L. Miao, W. Fan, D. Liu, F. Zhang, Y. Shi, and F. Guo, "Geochronology and geochemistry of the Hegenshan Ophiolitic complex: implications for late-stage Tectonic evolution of the inner Mongolia-Daxinganling Orogenic belt, China," *Journal of Asian Earth Sciences*, vol. 32, nos. 5–6, pp. 348–370, 2008.

[19] P. Jian, D. Liu, A. Kröner, et al., "Time scale of an early to mid-Paleozoic Orogenic cycle of the long-lived central Asian Orogenic belt, inner Mongolia of China: implications for Continental growth," *Lithos*, vol. 101, nos. 3–4, pp. 233–259, 2008.

[20] J. Tang, Z. Zhang, C. Ding, and B. Liu, "Felsic Dyke swarms from central inner Mongolian: implications for the Triassic Tectonic setting in the southeast central Asian Orogenic belt," *Lithos*, vols. 404–405, p. 106471, 2021.

[21] Z. Zhang, K. Li, J. Li, W. Tang, Y. Chen, and Z. Luo, "Geochronology and geochemistry of the Eastern Erenhot Ophiolitic complex: implications for the Tectonic evolution of the inner Mongolia-Daxinganling Orogenic belt," *Journal of Asian Earth Sciences*, vol. 97, pp. 279–293, 2015.

[22] J.-B. Zhou, J. Han, G.-C. Zhao, et al., "The Emplacement time of the Hegenshan Ophiolite: constraints from the Unconformably overlying Paleozoic strata," *Tectonophysics*, vol. 662, pp. 398–415, 2015.

[23] B. Xu, G. Zhao, J. Li, et al., "Ages and HF Isotopes of Detrital Zircons from Paleozoic strata in the Chagan Obo temple area, inner Mongolia: implications for the evolution of the central Asian Orogenic belt," *Gondwana Research*, vol. 43, pp. 149–163, 2017.

[24] Y. Li, G. Wang, M. Santosh, J. Wang, P. Dong, and H. Li, "Subduction initiation of the SE paleo-Asian ocean: evidence from a well preserved intra-Oceanic Forearc Ophiolite fragment in central inner Mongolia, North China," *Earth and Planetary Science Letters*, vol. 535, 2020.

[25] Q. W. Lu, Q. Tian, and G. H. Wang, "Stratigraphic subdivision and Geochronology study on the Baoligaomiao formation in the Abagaqi, inner Mongolia," *Western Resources*, no. 4, pp. 67–69, 2016.

[26] Y. Y. Wu, W. X. Ju, Y. X. Shao, and H. J. Jiang, "Stratigraphic division and age of upper Carboniferous-lower Permian Baoligaomiao formation in Qaganoboarea, Sonid left banner, inner Mongolia," *Geology in China*, vol. 42, no. 4, pp. 937–947, 2015.

[27] G. Sun, Y. Hu, S. Liu, S. Li, J. Fu, and L. Gao, "Featured Neoarchean Granitoid Association in the central North China Craton: an indicator of warm plate Subduction," *GSA Bulletin*, vol. 135, nos. 1–2, pp. 295–309, 2023.

[28] G. Zhang, T. Ireland, L. Zhang, Z. Gao, and S. Song, "Zircon geochemistry of two contrasting types of Eclogite: implications for the Tectonic evolution of the North Qaidam UHPM belt, northern Tibet," *Gondwana Research*, vol. 35, pp. 27–39, 2016.

[29] J. W. Zi, B. Rasmussen, J. R. Muhling, and I. R. Fletcher, "In situ U-PB and Geochemical evidence for ancient PB-loss during Hydrothermal alteration producing apparent young concordant Zircon dates in older Tuffs," *Geochimica et Cosmochimica Acta*, vol. 320, pp. 324–338, 2022.

[30] E. B. Watson and T. M. Harrison, "Zircon saturation Revisited: temperature and composition effects in a variety of Crustal Magma types," *Earth and Planetary Science Letters*, vol. 64, no. 2, pp. 295–304, 1983.

[31] W. Fang, L. Q. Dai, Y. F. Zheng, and Z. F. Zhao, "Molybdenum Isotopes in Mafic igneous rocks record slab Mantle interactions from Subarc to Postarc depths," *Geology*, vol. 51, no. 1, pp. 3–7, 2023.

[32] Q. H. Xiao, T. D. Li, G. T. Pan, et al, "Petrologic ideas for identification of ocean-continent transition: recognition of intra-Oceanic arc and initial Subduction," *Geology in China*, vol. 43, no. 3, pp. 721–737, 2016.

[33] M. J. Le Bas, "IUGS reclassification of the high-mg and Picritic volcanic rocks," *Journal of Petrology*, vol. 41, no. 10, pp. 1467–1470, 2000.

[34] A. Peccerillo and S. R. Taylor, "Geochemistry of Eocene Calc-alkaline volcanic rocks from the Kastamonu area, northern Turkey," *Contributions to Mineralogy and Petrology*, vol. 58, no. 1, pp. 63–81, 1976.

[35] J. B. Whalen, K. L. Currie, and B. W. Chappell, "A-type Granites: Geochemical characteristics, discrimination and Petrogenesis," *Contributions to Mineralogy and Petrology*, vol. 95, no. 4, pp. 407–419, 1987.

[36] O. Laurent, H. Martin, J. F. Moyen, and R. Doucelance, "The diversity and evolution of late-Archean Granitoids: evidence for the onset of "modern-style" plate Tectonics between 3.0 and 2.5Ga," *Lithos*, vol. 205, pp. 208–235, 2014.

[37] S. -s. Sun and W. F. McDonough, "Chemical and isotopic SYSTEMATICS of Oceanic Basalts: implications for Mantle composition and processes," *Geological Society, London, Special Publications*, vol. 42, no. 1, pp. 313–345, 1989.